Proton Conduction in Gramicidin A and in Its Dioxolane-Linked Dimer in Different Lipid Bilayers

Samuel Cukierman,* Edward P. Quigley,*# and David S. Crumrine#
*Department of Physiology, Loyola University Medical Center, and #Department of Chemistry, Loyola University Chicago, Maywood, Illinois 60153 USA

ABSTRACT Gramicidin A (gA) molecules were covalently linked with a dioxolane ring. Dioxolane-linked gA dimers formed ion channels, selective for monovalent cations, in planar lipid bilayers. The main goal of this study was to compare the functional single ion channel properties of natural gA and its covalently linked dimer in two different lipid bilayers and HCl concentrations (10–8000 mM). Two ion channels with different gating and conductance properties were identified in bilayers from the product of dimerization reaction. The most commonly observed and most stable gramicidin A dimer is the main object of this study. This gramicidin dimer remained in the open state most of the time, with brief closing flickers ($\tau_{closed} \approx$ 30 μs). The frequency of closing flickers increased with transmembrane potential, making the mean open time moderately voltage dependent (τ_{open} changed $\approx$ 1.43-fold/100 mV). Such gating behavior is markedly different from what is seen in natural gA channels. In PEPC (phosphatidylethanolamine-phosphatidylcholine) bilayers, single-channel current-voltage relationships had an ohmic behavior at low voltages, and a marked sublinearity at relatively higher voltages. This behavior contrasts with what was previously described in GMO (glycerylmonooleate) bilayers. In PEPC bilayers, the linear conductance of single-channel proton currents at different proton concentrations was essentially the same for both natural and gA dimers. g^{max} and K_D, obtained from fitting experimental points to a Langmuir adsorption isotherm, were ~1500 pS and 300 mM, respectively, for both the natural gA and its dimer. In GMO bilayers, however, proton affinities of gA and the dioxolane-dimer were significantly lower (K_D of ~1 and 1.5 M, respectively), and the g^{max} higher (~1750 and 2150 pS, respectively) than in PEPC bilayers. Furthermore, the relationship between single-channel conductance and proton concentration was linear at low bulk concentrations of H^+ (0.01–2 M) and saturated at concentrations of more than 3 M. It is concluded that 1) The mobility of protons in gramicidin A channels in different lipid bilayers is remarkably similar to proton mobilities in aqueous solutions. In particular, at high concentrations of HCl, proton mobilities in gramicidin A channel and in solution differ by only 25%. 2) Differences between proton conductances in gramicidin A channels in GMO and PEPC cannot be explained by surface charge effects on PEPC membranes. It is proposed that protonated phospholipids adjacent to the mouth of the pore act as an additional source of protons for conduction through gA channels in relation to GMO bilayers. 3) Some experimental results cannot be reconciled with simple alterations in access resistance to proton flow in gA channels. Said differences could be explained if the structure and/or dynamics of water molecules inside gramicidin A channels is modulated by the lipid environment and by modifications in the structure of gA channels. 4) The dioxolane ring is probably responsible for the closing flickers seen in the dimer channel. However, other factors can also influence closing flickers.

INTRODUCTION

Gramicidin A belongs to a family of highly hydrophobic pentadecapeptides produced by *Bacillus brevis* during the transition from its vegetative phase to sporulation. Gramicidin A molecules partition into lipid bilayers and form ion channels with biophysical properties similar to those observed in more complex ion channels present in membranes of excitable as well as nonexcitable cells. This functional property of gramicidin A has been used extensively to assess the complex relationship between the structure, biophysics, and physiology of ion channels in lipid bilayers (Andersen and Koeppe, 1992; Busath, 1993; Jordan, 1987; Koeppe and Andersen, 1996; Wallace, 1990). The primary structure of gramicidin A is (Sarges and Witkop, 1965)

HCO-L-Val-Gly-L-Ala-D-Leu-L-Ala-D-Val-L-Val-D-Val-L-

Trp-D-Leu-L-Trp-D-Leu-L-Trp-D-Leu-L-Trp-NH-$(CH)_2$-OH

Several investigators have contributed to the elucidation of the tridimensional structure of this unusual sequence of alternating L and D amino acids. Gramicidin A forms a right-handed, single-stranded $\beta^{6,3}$-helical motif in micelles and in solid state (Arseniev et al., 1985; Ketchem et al., 1993; Urry, 1971). By reasoning from the structure and energetics of gramicidin A molecules, Urry (1971) proposed that ionic channels are formed when two gramicidin A molecules are stabilized at their formyl N-termini by six intermolecular NH O hydrogen bonds inside a lipid bilayer. This proposal gained substantial support from different physicochemical measurements (see Andersen and Koeppe, 1992; Busath, 1993). An experimental approach that was essential to confirming Urry's original hypothesis was the chemical linkage of two gramicidin A molecules with a malonyl group (Bamberg and Janko, 1977; Urry et al., 1971). Malonyl-linked gramicidin A molecules formed ionic channels in lipid bilayers (Urry et al., 1971). More-

Received for publication 5 June 1997 and in final form 8 August 1997.

Address reprint requests to Dr. Samuel Cukierman, Department of Physiology, Loyola University Medical Center, 2160 South First Avenue, Maywood, IL 60153. Tel.: 708-266-9471; Fax: 708-216-6308; E-mail: scukier@luc.edu.

0006-3495/97/11/2489/14 $2.00

over, single-channel recordings demonstrated that malonyl-linked gramicidin A molecules existed predominantly in the open state (Bamberg and Janko, 1977). The main functional difference between malonyl-linked gramicidins and the dimeric association of gramicidin A molecules via hydrogen bonds was the difference in the opening-closing kinetics, as predicted by Urry (1971).

More recently, Stankovic et al. (1989) used a novel approach to covalently link two gramicidin A molecules. This time, however, a dioxolane ring was introduced as the molecular clip between two gramicidin A monomers. The rationale for the dioxolane ring was that this linker establishes a continuous and constrained rigid transition between the amino termini of two gramicidin A monomers. Therefore, a geometrical match between two gramicidin A molecules is provided, and most importantly, the β helicity of the dimer is preserved (Stankovic et al., 1989). The dioxolane-linked dimer has been used as the starting molecule to design and synthesize artificial ion channels with novel molecular and functional properties (Heinemann, 1990; Stankovic et al., 1990).

Studies of covalently linked gramicidin A molecules made a significant contribution to the understanding of the molecular architecture of gramicidin channels. In addition, they have also added to the understanding of mechanisms of protein folding in general (Stankovic et al., 1989, 1990; Urry et al., 1971). However, the functional implications of covalently linking gramicidin molecules were studied under a limited number of experimental conditions. To understand the functional implications of gramicidin's covalent linkers, it is essential to evaluate under different experimental conditions the properties of synthetic gramicidin A dimers and contrast their functional behavior with the gramicidin dimer formed via intermolecular hydrogen bonds. We reasoned that this approach could provide useful information toward a better understanding of structure-function relationships in ion channels.

In this study, we have synthesized and purified the dioxolane-linked gramicidin A dimer following procedures originally developed by Stankovic et al. (1989). Single-channel proton currents were measured in the dioxolane-linked gramicidin A dimers and compared under identical experimental conditions with proton currents in the naturally formed gramicidin A dimer. Experiments were performed in bilayers with different lipid compositions, and under a wide range of bulk $[H^+]$ ($[H^+]_{bulk}$: 10–8000 mM). Several reasons motivated us to study proton currents in gramicidin A channels. First, transmembrane proton currents occur in many different biological membranes (see DeCoursey and Cherny, 1994, 1997). Indeed, the translocation of protons through the F_0F_1-ATPase in the membrane of mitochondria and chloroplasts is one of the most essential phenomena in biology: proton movement is directly responsible for the efficient synthesis of ATP (Junge, 1989). Despite the ubiquitous nature of proton currents, their underlying molecular mechanisms are, in general, poorly understood (Akeson and Deamer, 1991; Deamer and Nichols, 1989; DeCoursey and Cherny, 1994; Paula et al., 1996; Prabhananda and Kombrabail, 1996). Second, it is generally accepted that proton movement in gramicidin A channels occurs via a Grotthuss mechanism (Finkelstein, 1987; Levitt et al., 1978; Myers and Haydon, 1972; Rosenberg and Finkelstein, 1978), i.e., translocation of protons along a file of water molecules inside the gramicidin pore occurs by breaking and reorganizing H^+ bonds between water molecules (Pomès and Roux, 1996; see Discussion). Consequently, the study of proton movement in different gramicidin A channels offers an opportunity to gain insight to the functional properties of water molecules inside gramicidin pores, and how this movement can be modulated by different molecular groups. Little is known about the influence of the chemical environment on the organization of water molecules inside ionic channels. Third, gramicidin exhibits an "abnormally" high single-channel conductance of protons (Akeson and Deamer, 1991; Heinemann, 1990; Hladky and Haydon, 1972). This has the clear advantage of allowing single-channel recordings with a large signal-to-noise ratio, even with conventional planar bilayer methods without having to resort to more sophisticated methods of recording (see Andersen, 1983a; Sigworth et al., 1987). The unusually large signal-to-noise ratio obtained in our experiments allowed a more reliable comparative analysis of gating between different gramicidin A molecules.

MATERIAL AND METHODS

Lipid bilayers

Membranes were formed onto a 0.1-mm-diameter hole drilled into a polystyrene partition separating two 3-ml HCl solutions. Two different lipid compositions were used:

1. 1-Palmitoyl-2-oleoyl-phosphatidylethanolamine (PE) and 1-palmitoyl-2-oleoyl-phosphatidylcholine (PC), PE:PC:4:1 (~60 mM in decane). Synthetic PE and PC were obtained from Avanti Lipids (Alabaster, AL). Gramicidin A channels are seldom studied in PEPC bilayers. Two main reasons led us to choose this lipid composition. First, PEPC bilayers are extremely stable and tolerant to our experimental conditions, in which $[H+]_{bulk}$ up to 8000 mM were used. Even at this high concentration, PEPC membranes remained stable at high transmembrane potentials (400 mV). Second, and for reasons that will be examined in a future study (Quigley et al., manuscript in preparation), PE increases the frequency of closures in dioxolane-linked dimers, thus allowing a precise determination of open-channel currents at different voltages. PE has previously been shown to decrease the mean open time of naturally occurring gramicidin A channels (Neher and Eibl, 1977; Maer et al., 1997).

2. Glycerylmonooleate (GMO) (Nu-Check, Elysian, MN; ~60 mM in decane). To compare some of our results with those in the literature (Akeson and Deamer, 1991; Heinemann, 1990; Stankovic et al., 1989), experiments were also performed with GMO bilayers. Unfortunately, it was not possible to study single-channel currents at high (>150 mV) voltages in GMO. GMO bilayers are significantly less stable (see Akeson and Deamer, 1991) than PEPC bilayers, and they rupture at those high voltages.

Solutions

Solutions were made by diluting concentrated stock solutions of HCl (Fischer Scientific, Chicago, IL) with distilled and deionized water (Nano-

pure water; Barnstead, Dubuque, IA). Single-channel currents were measured in symmetrical (same concentration of HCl on both sides of the membrane) as well as in asymmetrical conditions (HCl gradient across the membrane).

Gramicidin A and its covalently linked dimers were stored in methanol ($\sim 2 \times 10^{-10}$ M) at −30°C. To obtain channel incorporation in bilayers, 5 μl of methanol solution was added to only one side of the membrane (concentration of gramicidin A in the bath was ~0.4 pM). Within the time frame of a typical experiment (10–30 min), this concentration allowed the incorporation of only one to three channels into the bilayer. All experiments were performed at room temperature (22–23°C).

Electrophysiology

HCl solutions on both sides of the membrane were connected via 3 M KCl agar bridges and Ag/AgCl wires to a List EPC-7 patch-clamp amplifier (List Electronics, Darmstadt, Germany). One side of the membrane was connected to ground, whereas voltages and transmembrane currents were applied or measured on the other side (virtual-ground configuration). Transmembrane currents were recorded in a conventional videotape recorder via a Neurocorder DR-384 (Neurodata Instruments, New York), using the 10 kHz filter of the List amplifier. Experiments were analyzed offline. At the end of each experiment, the lipid membrane was broken and voltages between electrodes were measured in the absence of applied voltage. For experiments in symmetrical solutions, an experiment was not analyzed if the voltage between electrodes was more than ±3 mV. Offset voltages less than or equal to ±3 mV were added as corrections to applied voltages during the experiment. Transmembrane voltages applied during experiments in asymmetrical solutions were corrected in full for the offset voltage measured at the end of the experiment. Single-channel recordings were played back from the VCR and filtered with an 8-pole low-pass Bessel filter (Frequency Devices, Haverhill, MA). AD conversion was performed with a PC-486, using pClamp hardware and software (Axon Instruments, Foster City, CA). Settings of the low-pass filter as well as the AD sampling rates are given in the Results. Single-channel analyses and nonlinear regression fittings of experimental points were performed with pClamp (Axon Instruments) or Sigmaplot (Jandel Scientific, San Rafael, CA).

Control experiments

Two different types of control experiments were performed. 1) Because lipid bilayers have a relatively high permeability to H^+ (see Deamer and Nichols, 1989), it was important to determine alterations in transmembrane conductance in the absence of gramicidin A channels. The single-channel activity shown in this study was never observed without gramicidin A channels added to HCl solutions. Moreover, without gramicidin A channels added to solutions, typical lipid bilayers had time-independent resistances of ~100 GΩ, even with the highest concentration of HCl. 2) Additions of methanol (without gramicidin A) to the bath chamber did not cause alterations in transmembrane conductance. Therefore, single-channel currents reported in this study were caused by gramicidin A channels incorporated into lipid bilayers.

Synthesis and purification of dioxolane-linked gramicidin A dimers

Fig. 1 shows the basic sequence of different chemical steps used to synthesize the dioxolane-linked gramicidin A. Stankovic et al. (1989, 1990) should be consulted for more experimental details. In brief, gramicidin A was purified from the commercially available mixture of isomers (gramicidins A, B, C) by flash chromatography on silica gel eluted with chloroform/methanol/water/acetic acid. Separation of different gramicidins was done with high-performance thin-layer chromatography. The *N*-formyl protecting group of gramicidin A was removed by acid hydrolysis. Desformylated gramicidin A was lyophilized and purified on an AG11A8

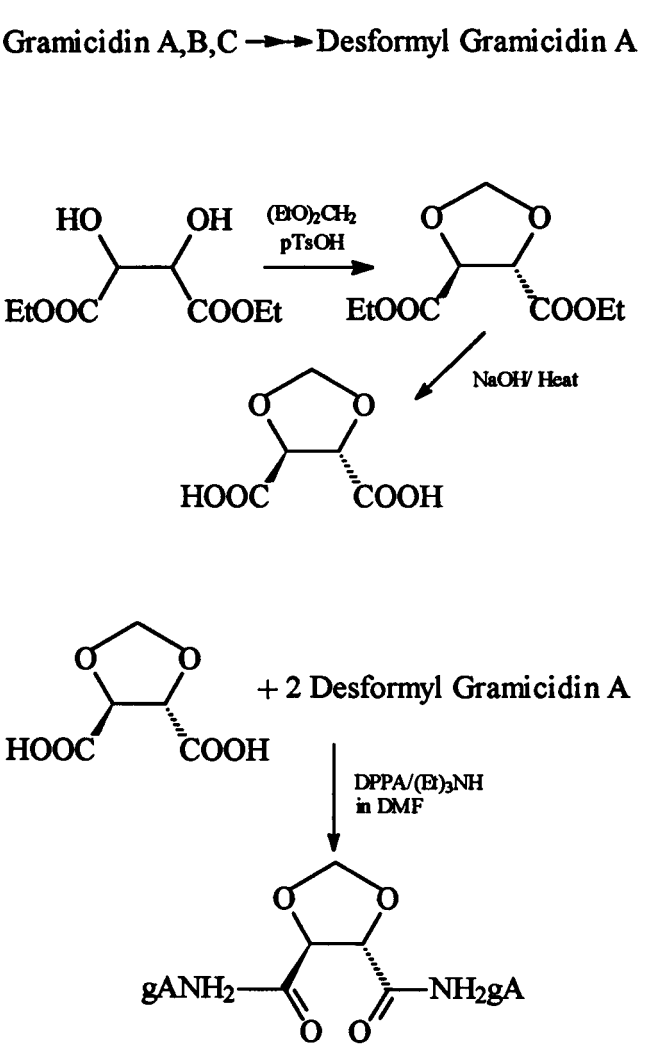

FIGURE 1 Three main steps in the process of chemical synthesis of dioxolane-linked gramicidin A dimer. See text for description.

column. The dioxolane ring linking group was synthesized from diethyl tartrate and diethoxymethane. The closure of the dioxolane ring produced two stereoisomers (*R,R* and *S,S*), which differed in the chirality of positions 2 and 3 of the tartaric acid. Dioxolane-linked dimer products were purified with silica gel column chromatography and assessed by nuclear magnetic resonance, thin-layer chromatography, and infrared spectroscopy. The diethyl tartrate acetal was subsequently saponified and acidified to yield the unprotected dicarboxylic acids. Dicarboxylic acid was reacted with two equivalents of the desformyl gramicidin A. Peptide bond formation between the carboxylic acid of the dioxolane linker and the free N-terminals of gramicidin was catalyzed with triethylamine and diphenylphosphoryl azide in dimethylformamide. Gramicidin A dimers were purified by high-performance liquid chromatography on a C18 reversed-phase column eluted with methanol/water (Hewlett Packard C18 spherisorb, 4 × 250 mm). Multiple passes yielded pure samples for spectroscopic and biophysical studies. Dioxolane-linked gramicidin dimers were characterized by 1-D proton-nuclear magnetic resonance spectroscopy (Varian 300 and 400 MHz).

Channel nomenclature

The following conventions for gramicidin A channels are used in this study. gA···gA denotes the naturally occurring gramicidin A channel that is

formed by hydrogen bonds in the lipid bilayer. gA~D_1~gA and gA~D_2~gA are the two different types of channels identified from the final product of reaction linking two gramicidin A channels with a dioxolane ring. This classification is operational, and at this point, no attempts have been made to correlate gA~D_1~gA and gA~D_2~gA with *S,S* or *R,R* stereoisomers (Stankovic et al., 1989; see Discussion).

Surface charge effects in phospholipids

As will be demonstrated in this study, proton conduction in gramicidin A as well as in its dioxolane-linked dimer is profoundly influenced by the composition of bilayers. One essential difference between GMO and phospholipids is that phosphate groups in PE and PC can be protonated. PE and PC are zwitterions, and protonation of the negatively charged phosphate makes these phospholipids acquire a net positive charge that is present in the ammonium group. As $[H^+]_{bulk}$ increases, phosphate protonation increases, and so does the net positive surface charge density of PEPC bilayers. The increased positive surface charge density in bilayers will change the concentrations of ions at the membrane-solution interface. Concentrations of protons and Cl^- at the membrane-solution interfaces ($[H^+]_0$ and $[Cl^-]_0$) will decrease and increase, respectively, in relation to their bulk concentrations. Because the openings of gramicidin A channels are likely to see $[H^+]_0$ instead of $[H^+]_{bulk}$, it is important to calculate the concentration of $[H^+]_0$ at the PEPC/solution interface. This will allow a more appropriate comparison between conductance data obtained in GMO versus PEPC bilayers. The combination of Eqs. 1 (Grahame equation based on a Gouy-Chapman model) and 2 (combination of a Langmuir adsorption isotherm with Boltzmann equations) allows the calculation of $[H^+]_0$ (see Cukierman, 1991, 1993, and Israelachvili, 1992, for a more detailed description of the equations and model used here):

$$\sigma^2 = (2 * \epsilon_0 * \epsilon * R * T) * [H^+]_{bulk} * [\exp(zV_0F/RT) + \exp - (zV_0F/RT) - 2] \quad (1)$$

$$\sigma = \sigma^{max} * \{[K_A * [H^+]_{bulk} * \exp(-zV_0F/RT)]/ [1 + K_A * [H^+]_{bulk} * \exp(-zV_0F/RT)]\} \quad (2)$$

In the equations above, σ is the surface charge density in C/m^2 at a given $[H^+]_{bulk}$ (σ^{max} = 0.267 C/m^2, which is equivalent to one elementary positive charge per phospholipid headgroup surface of 60 A^2), ϵ_0 is the permittivity of free space (8.85×10^{-12} $C^2/N/m^2$), ϵ is the dielectric constant of water (78), V_0 is the voltage at the membrane solution interface, and K_A is the phospholipid-proton association constant (10 M^{-1}; see Marsh, 1990). *R*, *T*, *z*, and *F* have their usual meanings.

Fig. 2 shows the effects of different $[H^+]_{bulk}$ on V_0 and σ/σ^{max} (*left panel*). As $[H^+]_{bulk}$ increases, the positive surface charge density of the bilayer approaches a saturating limit of 0.267 C/m^2 (*dotted curve*). Notice that this is a simple adsorption isotherm corrected for surface charge effects. The increase in $[HCl]_{bulk}$ has two simultaneous and opposing effects on V_0. At relatively low concentrations, an increase in $[H^+]_{bulk}$ will increase V_0 because of an increased protonation of phospholipids. However, as $[HCl]_{bulk}$ increases, so will the screening effect of ionic strength on V_0: $[Cl^-]_0$ increases and screens the local potential at the membrane/solution interface. This will eventually result in a decline of V_0 (*solid curve*). The graph in the right panel of Fig. 2 shows the relationship between $[H^+]_0$ and $[H^+]_{bulk}$. This was calculated by using the Boltzmann relationship $[H^+]_0 = [H^+]_{bulk} \exp(-zV_0F/RT)$, with V_0 obtained from the graph in the left panel. It should be mentioned that one of the implicit assumptions of our model is that gramicidin channels sense the concentration of ions at the membrane-solution interface. It is possible, but not likely from geometrical considerations of gramicidin and bilayer lengths, that the mouths of the gramicidin A pore see the ionic concentrations at several Debyes away from the plane of the bilayer. The qualitative nature of the conclusions presented in this study, however, is not challenged by this factor.

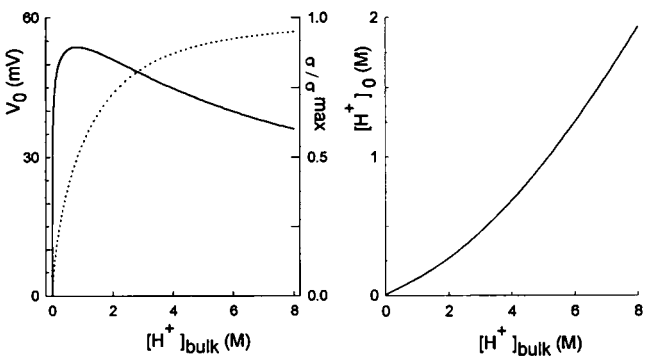

FIGURE 2 (*Left*) Calculation of the electrostatic potential at the membrane-solution interface (V_0, ——), and the relative surface charge density (σ/σ^{max}, – – –) as a function of proton bulk concentration ($[H^+]_{bulk}$). (*Right*) Relationship between $[H^+]_0$ and $[H^+]_{bulk}$. See text for details.

RESULTS

Two different channel types in lipid bilayers were identified from the reaction products of dimerization of gramicidin A

Fig. 3 shows single-channel recordings of gA···gA (*A*), and gA~D_1~gA (*B*) in 500 mM $[H^+]_{bulk}$ (62 mM $[H^+]_0$) at a 100-mV applied potential. With a gA···gA concentration of ~0.4 pM in one HCl compartment, and within the average duration of an experiment, the gating pattern of gA···gA illustrated in Fig. 3 *A* was commonly observed, and is similar to many results previously described by different laboratories (see Andersen, 1984). Opening and closing of gA···gA channels is caused by association and dissociation of gramicidin A monomers in the lipid bilayer. Notice that the open state of gA···gA channels did not have brief closures. The relatively short open times of gA···gA shown in this as well as in other figures in this study have been attributed to the presence of PE in lipid bilayers (see Neher and Eibl, 1977; Maer et al., 1997). By contrast, completely

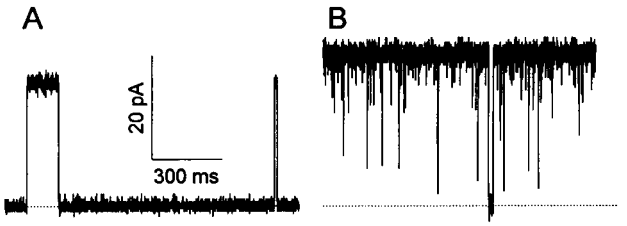

FIGURE 3 Single-channel recordings of gA···gA (*A*) and gA~D_1~gA (*B*) in PEPC lipid bilayers. Membrane potential was 100 mV, and single-channel recordings were obtained in 500 mM HCl ($[H^+]_0$ = 62 mM). The closing state, or zero current level, for both gramicidin A channels is identified by dotted lines. Upward and downward current deflections correspond to opening and closing of channels, respectively. Single-channel conductances were 247 pS (*A*) and 260 pS (*B*). In both panels, single-channel recordings were low-pass Bessel filtered at 2 kHz and digitized at 4 kHz. Calibration marks in *A* apply to both panels.

different types of channels were observed in lipid bilayers when aliquots of a methanol solution containing the products of the dioxolane-linked gramicidin reaction were added to HCl solutions. The most common type of channel observed in our experiments was named gA~D_1~gA and is illustrated in Fig. 3 *B*. Whereas Fig. 3 *A* shows that gA···gA had a relatively short and stable open time, Fig. 3 *B* shows a channel (gA~D_1~gA) that remained predominantly in the open state with very brief excursions into the closed state (closing flickers). Most of these closing flickers were not completely resolved, even at 10 kHz (see other single-channel recordings in different figures). The gating pattern of gA~D_1~gA shown in Fig. 3 *B* lasted for the entire length of experiment. The channel shown in Fig. 3 *B* is the main subject of the present study.

gA~D_1~gA was not the only ionic channel seen in lipid bilayers that originated from the products of dimerization reaction of gramicidin A. Another channel, gA~D_2~gA, with a significantly smaller conductance and a different gating mode, was also observed. In Fig. 4 *A* this channel is shown in a lipid bilayer that also contained a gA~D_1~gA channel. There are two major differences between gA~D_1~gA and gA~D_2~gA channels: 1) Whereas gA~D_1~gA remained essentially in the open state with closing flickers (five of these brief closures can be clearly identified in Fig. 4 *A*), gA~D_2~gA remained predominantly in the closed state with relatively long-duration openings. 2) For the experiment shown in Fig. 4 *A*, the proton conductances of gA~D_1~gA and gA~D_2~gA were 1026 pS and 689 pS, respectively. In Fig. 4 *B*, the gA~D_2~gA conductance channel is shown by itself in a different experiment. gA~D_1~gA and gA~D_2~gA could be observed together in the same lipid bilayer or isolated. When these channels were seen together in a lipid bilayer, no preferential order of appearance in the membrane was noticed. The experimental observations suggest that the two synthetic gramicidin dimers are independent molecules. An interesting feature of gA~D_2~gA was that it was not stable in lipid bilayers. gA~D_2~gA incorporated into the bilayer, gated with the typical behavior shown in Fig. 4, and "disappeared" after 1–3 min. This characteristic prevented us from studying in detail its functional properties. In summary, gA~D_1~gA was observed in every single experiment with GMO or PEPC bilayers, and its gating characteristic illustrated in this study was stable throughout the entire duration of the experiment. On the other hand, gA~D_2~gA was not observed in every experiment, and when it was, it remained "silent" (did not open or was not present in bilayer) for most of the duration the experiment.

Fig. 5 shows an infrequent but consistently observed substate of gA~D_1~gA channels in different experimental conditions. Whereas gA···gA channels are known to have different conductance substates (Busath and Szabo, 1981; see Fig. 7), gA~D_1~gA channels displayed only one substate. Recordings in Fig. 5 show that this substate is characterized by a conductance that is ~25–35% of the full open state, and, most interestingly, by the lack of closing flickers. This substate can last for several hundred milliseconds.

Observations shown in Figs. 3–5 are representative of a total of more than 40 h of single-channel recordings in different lipid bilayers and HCl concentrations with the products of reaction linking gramicidin A channels with a dioxolane ring. gA~D_1~gA and gA~D_2~gA were the only channel types originating from the product of dimerization of gramicidin A.

The mean open time of gA~D_1~gA decreases with membrane potential

The frequency of closing flickers increased with membrane voltage. Fig. 6 shows histograms of single-channel open and closed dwell times at different transmembrane voltages. Analyses of dwell-time distributions were only performed

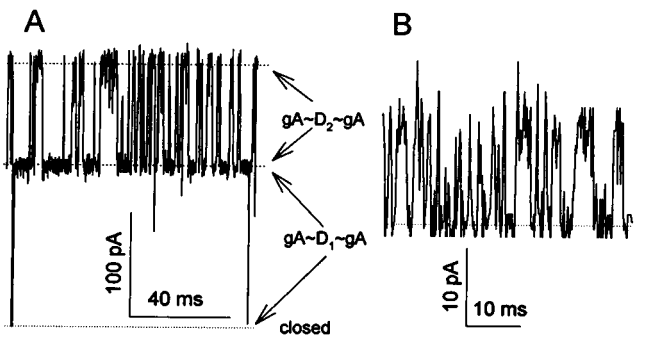

FIGURE 4 Single-channel recordings of gA~D_2~gA in different lipid bilayers and experimental conditions. (*A*) gA~D_1~gA and gA~D_2~gA in the same PEPC bilayer. Zero current levels in both recordings are indicated by dotted lines. The membrane potential was 150 mV, and $[H^+]_{bulk}$ was 4000 mM ($[H^+]_0$ = 685 mM). Single-channel recordings were low-pass filtered at 4 kHz and digitized at 20 kHz. (*B*) Single-channel recordings were obtained from a GMO bilayer at a $[H^+]_{bulk}$ of 1 M ($[H^+]_0$ = 122 mM) at 60 mV. The single-channel conductance was 235 pS. Recording was low-pass Bessel filtered at 5 kHz and digitized at 10 kHz.

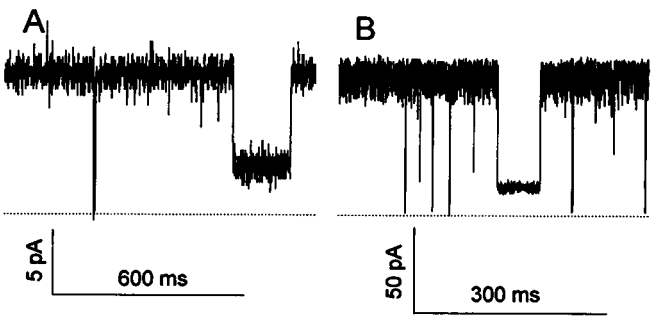

FIGURE 5 Single-channel recordings of gA~D_1~gA in different concentrations of HCl, showing the only conductance substate identified. (*A*) Recordings were obtained in 125 mM bulk HCl ($[H^+]_0$ = 19.5 mM), at 100 mV, and in a PEPC bilayer. Single-channel currents were low-pass filtered at 2 kHz and digitized at 5 kHz. (*B*) Experimental conditions: 8 M HCl ($[H^+]_0$ = 1935 mM), PEPC bilayer, 100 mV. Membrane currents were low-pass filtered at 2 kHz and digitized at 8 kHz.

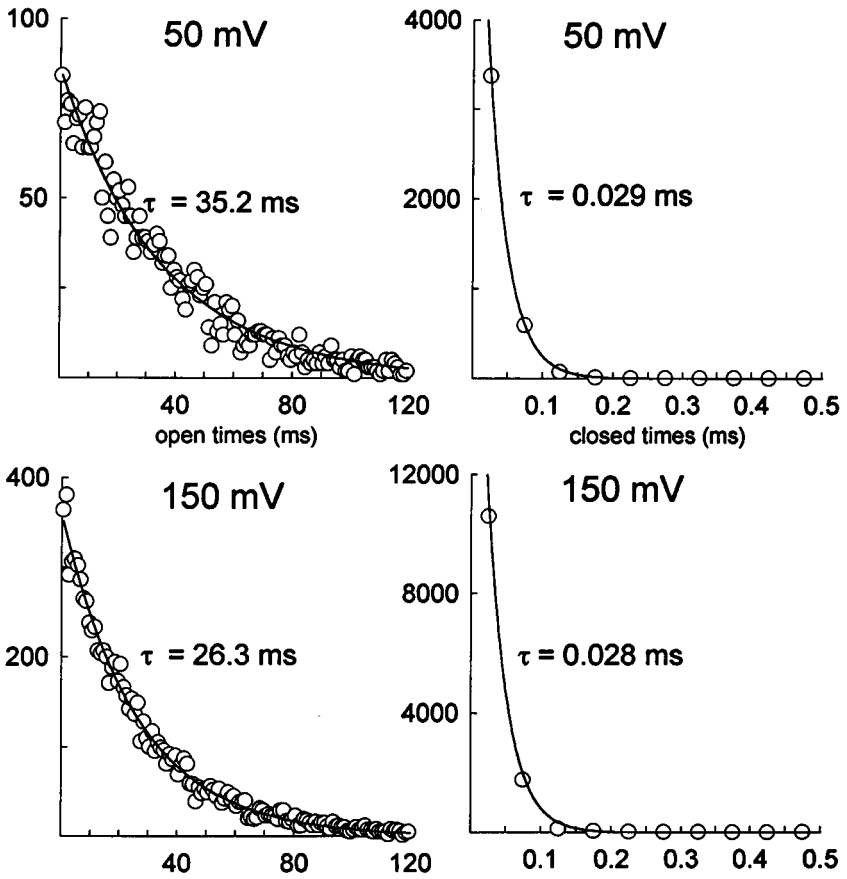

FIGURE 6 Histogram distributions of open and closed dwell times at different voltages. Open and closed states were identified by a threshold located at a level of 50% of the current corresponding to the full open state of the channel. Single-channel events were binned at 50 μs and 1 ms for the closed and open dwell states, respectively. A Levenberg-Marquardt least-squares fitting method was used to fit experimental points with single exponentials, the time constants of which are indicated on each graph. Fitting these curves with more than one exponential did not significantly improve the quality of fit, as evaluated by eye inspection and conventional statistical parameters (sum of squared errors, standard deviation of function, *F*-statistics, and convergence criteria).

in membranes that contained only a single channel. The criterion for identifying a single channel was the absence of multiple conductance states in the current recording. Whereas the mean closed time remained essentially unchanged at 50 or 150 mV, the mean open time decreased from 35 (50 mV) to 26 ms (150 mV). This result is representative of three different experiments (two in PEPC and one in GMO bilayers). The means ± SEM were 40 ± 6 ms (at 50 mV) and 28 ± 4 ms (at 150 mV). Mean closed times were essentially unaltered in other experiments. Because distribution histograms of both open and closed events could be fitted well by single exponentials, a minimum gating model for gA~D_1~gA is consistent with a single open and a single closed state. The mean open time of gA~D_1~gA decreased because the frequency of closing flickers in gA~D_1~gA increased. This increase could not be attributed to membrane instability at higher voltages. Bilayers without channels did not have flickers at high voltages (>100 mV). Furthermore, the open state of gA···gA channels did not have closing flickers at high voltages (see Fig. 7, for example). It is interesting to note that closing flickers in gA···gA were observed in CsCl solutions and in GMO bilayers (Ring, 1986; Sigworth et al., 1987). Different bilayers and/or permeating ions must have an effect on the stability of the open state of gA···gA (see Discussion).

Single-channel proton currents in gA···gA and gA~D~gA

Fig. 7 shows representative single-channel H^+ currents in gA···gA (*left column*) and gA~D_1~gA (*right column*) at different $[H^+]_0$ indicated for each row. Recordings were obtained at 100 mV. In Fig. 8, single-channel current-voltage (*I-V*) relationships are illustrated for gA~D_1~gA (*upper row*) and gA···gA (*lower row*) at $[H^+]_0$ concentrations of 9.8 mM (*left column*) or 1578 mM (*right column*). Single open-channel currents were measured from closing events lasting for several milliseconds. At relatively low voltages, the initial component of *I-V* plots could be approximated by a straight line. As $[H^+]_0$ increased, so did the initial range of voltages that fell in a straight line in *I-V* plots. However, at higher voltages, single-channel currents in both gA···gA and gA~D_1~gA departed considerably from linearity. *I-V* plots under different proton concentrations showed a strong sublinear behavior, with saturation of single-channel currents occurring at very high voltages.

In Fig. 9 the linear component of proton conductance was plotted against different $[H^+]$ for both gA~D_1~gA (*left*

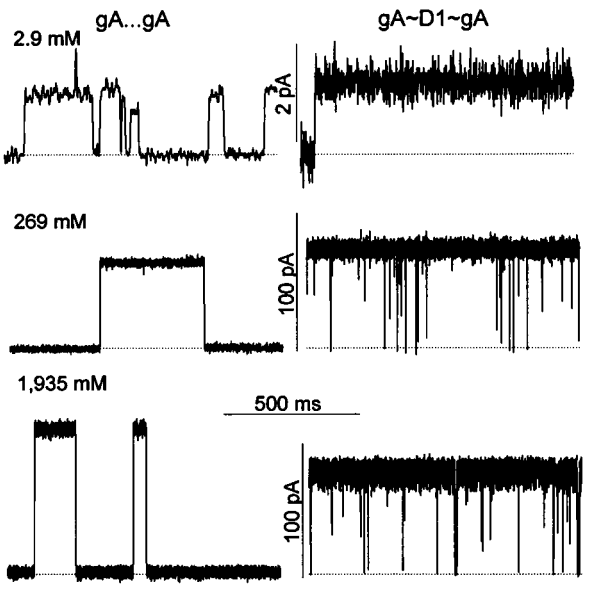

FIGURE 7 Representative single-channel H^+ currents in gA···gA (*left column*) and gA~D_1~gA (*right column*) at 100 mV, under different $[H^+]_0$ in PEPC bilayers. Recordings in 2.9 mM $[H^+]_0$ (10 mM $[H^+]_{bulk}$, *upper row*) were low-pass filtered at 0.25 kHz and digitized at 1 kHz. In 269 mM $[H^+]_0$ (2000 mM $[H^+]_{bulk}$) the low-pass filter setting (and AD sampling rate) were 2 kHz (4 kHz) and 5 kHz (10 kHz) for single-channel recordings obtained from gA···gA and gA~D_1~gA, respectively. In 1935 mM $[H^+]_0$ (8 M $[H^+]_{bulk}$), the filter and AD sampling rate settings for single-channel recordings were 4 kHz (10 kHz) for gA···gA and 4 kHz (8 kHz) for gA~D_1~gA. Notice the differences between conductances in 269 and 1935 mM $[H^+]_0$ for gA···gA and gA~D_1~gA.

panel) and gA···gA (*right panel*). Experiments were performed either in PEPC (*open symbols*) or in GMO (*filled symbols*) bilayers. Note that data in PEPC bilayers were plotted in two different ways: 1) with corrections for surface charge effects at the membrane/solution interface (*open circles* or *squares*, g versus $[H^+]_O$) or 2) without corrections for surface charge effects (*triangles*, g versus $[H^+]_{bulk}$; see Fig. 2). In PEPC bilayers (2.9–1, 250 mM $[H^+]_0$ range), proton conductances of gA~D_1~gA and gA···gA have similar concentration-dependent properties. Single-channel conductances in PEPC bilayers could be fit well with a simple Langmuir isotherm (Fig. 9, *insets, solid curves*),

$$g = g^{max} * [H^+]_0/(K_D + [H^+]_0) \quad (3)$$

where g is the single-channel proton conductance, and K_D is the dissociation constant of protons from phospholipids (see Discussion). g^{max} and K_D for gA~D_1~gA and gA···gA were 1546 ± 31 and 1469 ± 65 pS, and 280 ± 16 and 300 ± 45 mM, respectively. These constants apply only to data corrected for surface charge effects (*open circles* and *squares*). Equation 3 also provided adequate fits to the triangles, which are the open circles and squares plotted against $[H^+]_{bulk}$ (without correction for surface charge effects at the membrane/solution interface; results not shown). An interesting experimental finding was that at concentrations above 1250 mM $[H^+]_0$ (6 M $[H^+]_{bulk}$), a significant decline in proton conductance was consistently noticed for gA~D_1~gA, but not for gA···gA. This conductance decline occurred in PEPC bilayers only (see below).

Fig. 9 also shows that lipid bilayers had a significant effect on proton conductance in gramicidin A channels. In GMO bilayers, single-channel proton conductance increased in an approximately linear fashion in 10–2000 mM $[H^+]_0$ (with GMO bilayers, $[H^+]_0 = [H^+]_{bulk}$). The g-$[H^+]_0$ relationship was steeper in gA~D_1~gA (1072 pS/M) than in gA···gA (723 pS/M). On the other hand, g^{max} values were considerably larger in gA···gA (~2150 pS) than in gA~D_1~gA (~1750 pS). Note that g^{max} values were larger in GMO than in PEPC bilayers. Our conductance measurements with GMO bilayers are in good agreement with previous results (Akeson and Deamer, 1991). Moreover, a linear relationship between proton conductance and $[H^+]_0$ has also been shown for gA···gA in GMO bilayers (see figure 4 in Akeson and Deamer, 1991). Equation 3 above did not provide a tolerable fit to different values of g in GMO bilayers. Finally, it should be noted that affinities of both gA~D_1~gA and gA···gA for protons are considerably higher in PEPC bilayers (see *insets* in Fig. 9).

At relatively high transmembrane voltages, single-channel currents in both gA···gA and gA~D_1~gA were voltage independent (Fig. 8). At $[H^+]_0 < 1250$ mM, saturating single-channel currents were larger in gA~D_1~gA than in gA···gA. In 9.8 mM $[H^+]_0$ (Fig. 8), single-channel proton currents saturated at ~9.2 pA for gA~D_1~gA, and at 7.2 pA for gA···gA. At $[H^+]_0$ above 1250 mM, however, voltage-independent single-channel currents were significantly larger in gA···gA than in gA~D_1~gA. In 1578 mM $[H^+]_0$, limiting proton currents were 328 and 265 pA for gA···gA and gA~D_1~gA, respectively. This observation relates to the fact that an overall significant decline in single-channel conductance occurred at $[H^+]_0$ above 1250 mM for gA~D_1~gA (see Figs. 7 and 8).

Selectivity of gramicidin A channels is maintained under different HCl concentrations

It was important to determine whether the selectivity of gramicidin A channels was maintained under different concentrations of HCl. Fig. 10 shows two *I-V* plots measured under different asymmetrical conditions ($[H^+]_{bulk}$ values: *circles*, 846//250 mM; *squares*, 1455//1000 mM). The reversal potentials (zero current voltage) for these as well as for many other experiments in asymmetrical conditions were close to the calculated equilibrium electrochemical potential for H^+ (E_H) or OH^- (E_{OH}) (see Fig. 10 legend). Because $E_H = E_{OH}$, the possibility exists that a combination of H^+ and OH^- currents was actually measured in our experiments. It is likely, however, that single-channel currents in this study are due to proton movement: 1) gramicidin channels were selectively permeable to monovalent cations under a wide range of experimental conditions (note that Cl^- in our experimental conditions did not permeate

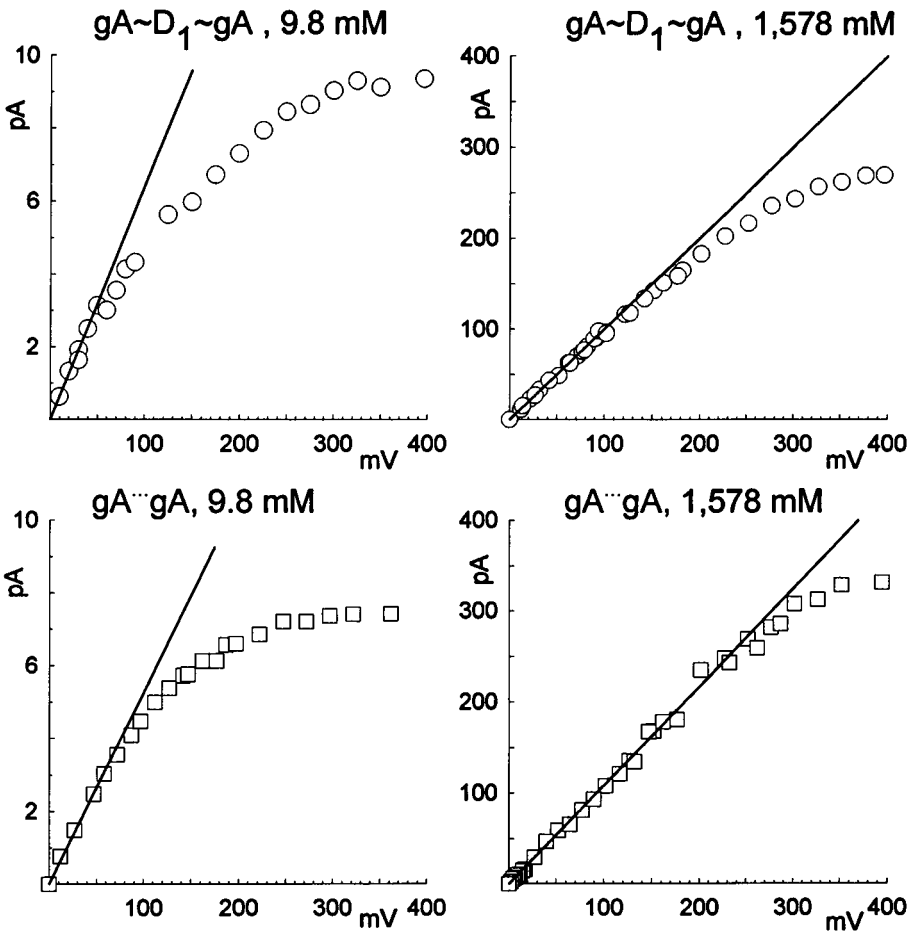

FIGURE 8 Single-channel current-voltage relationships in different gramicidin A channels in different HCl concentrations. Single-channel conductances of the initial linear part of curves were 60 and 1037 pS (gA~D_1~gA in 9.8 mM ($[H^+]_{bulk}$ = 50 mM) and 1578 mM ($[H^+]_{bulk}$ = 7000 mM), respectively), and 54 and 1085 pS (gA···gA in 9.8 and 1578 mM $[H^+]_o$, respectively).

channels), and 2) an increase in $[H^+]$ (decrease in $[OH^-]$) caused an increase in proton conductance in different gramicidin A channels.

DISCUSSION

Dioxolane-linked gramicidin A channels: comparison between different experimental results

Two different dioxolane-linked gramicidin A dimers were originally identified in GMO bilayers by Stankovic et al. (1989). These channels were characterized as the stereoisomers *S,S* and *R,R* of the dimer (see Fig. 1 and Methods). In 640 mM KCl, the *S,S* dimer had a long-lived open state (30 pS at 200 mV) and did not close to the zero conductance level. By contrast, the *R,R* dimer had a smaller single-channel conductance (6 pS at 200 mV) with fast closing flickers. A moderate sublinearity was present in *I-V* plots obtained in 640 mM KCl for both gA···gA and the *S,S* dimer. By contrast, the *I-V* relationship for the *R,R* dimer was strongly supralinear. In a later publication, Stankovic et al. (1990; see also Heinemann, 1990) reported that both the *S,S* and *R,R* dimers had conductances of ~75–90 pS in 40 mM H^+ (GMO bilayers at 200 mV). Although these single-channel conductances in HCl are certainly comparable with the proton conductance of the gA~D_1~gA channel (see Fig. 9), there are interesting experimental discrepancies between our data: 1) A channel with the gating characteristic of the *S,S* dimer in 40 mM HCl (Stankovic et al., 1990) was not observed in our experiments. Both gA~D_1~gA and gA~D_2~gA had well-defined transitions between the open and closed states under a wide range of voltages in both GMO or PEPC bilayers. We have failed to observe channels that remained open without closing flickers. On the other hand, Stankovic et al. (1989, 1990) have not reported a channel similar to gA~D_2~gA in either HCl (40 mM) or KCl (640 mM). 2) The ratio between proton conductances of gA~D_2~gA and gA~D_1~gA at the same proton concentration was ~0.65 (see Fig. 4). By contrast, the *R,R* and *S,S* dimers had similar conductances in 40 mM HCl (Stankovic et al., 1990). 3) gA~D_1~gA had a long and quiet duration conductance substate. Conductance substates were not reported for the *R,R* or the *S,S* dimers.

Even though it may well be that gA~D_1~gA and the *R,R* dimer are the same channel (see section on gating below), it is not possible at this stage to unequivocally correlate the *R,R* and *S,S* dimers with gA~D_1~gA and gA~D_2~gA channels. This was the main reason for adopting a different nomenclature for the dimer channels reported in this study. It is hoped that future work under different experimental

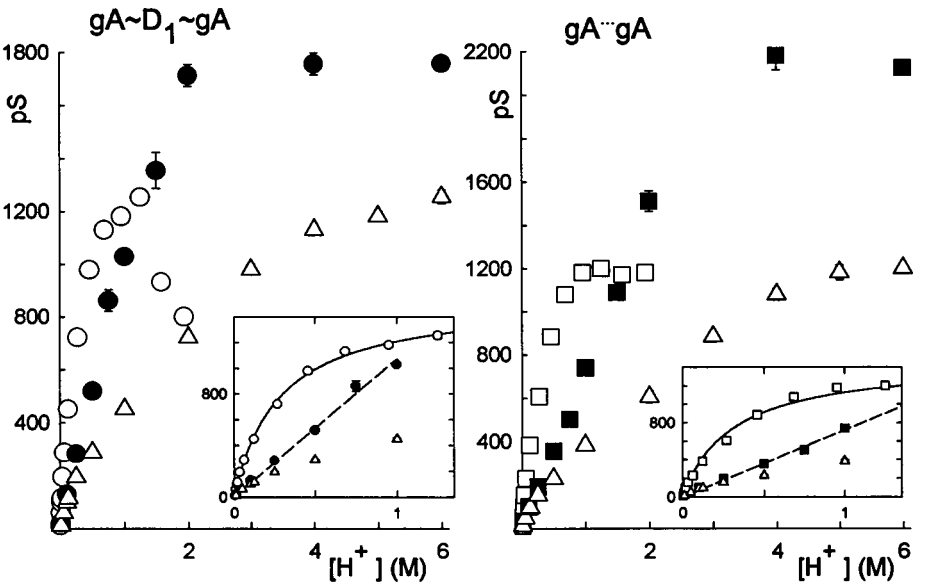

FIGURE 9 Conductance-$[H^+]$ relationships for gA~D_1~gA (●, GMO bilayers; ○, △, PEPC bilayers) and gA···gA (■, GMO bilayers; □, △, PEPC bilayers). Single-channel proton conductances plotted in this figure were measured from the linear component of conductance at relatively low applied voltages (zero current conductance; see Fig. 8). Each point represents the mean ± SEM of 4–26 different observations. Insets in both graphs amplify the region between 1 and 1.5 M $[H^+]_o$. Solid curves in the insets were best fits to Eq. 3 in text. Dashed lines were drawn from linear regression analysis. The slopes are 1072 and 723 pS/mol for gA~D_1~gA and gA···gA, respectively. Open circles and squares were plotted against $[H^+]_O$ (see Fig. 2). Triangles are the open circles (or open squares) plotted against $[H^+]_{bulk}$ in PEPC bilayers, i.e., triangles are open circles or squares that were not corrected for surface charge effects in PEPC bilayers (see Fig. 2 and text).

conditions will clarify discrepancies, if any, between data obtained by different laboratories.

Gating of dioxolane-linked gramicidin A dimers

Our experiments in PEPC bilayers clearly showed that with H^+ as the conducting ion, the open state of gA···gA channels has no closing flickers. In contrast, gA~D_1~gA, which was studied in experimental conditions identical to those of gA···gA, exhibited intense flickering activity. This result suggests that changes in the position of dioxolane ring inside the dimer could cause channel closures (Stankovic et al., 1989, 1990). In one of the first attempts to study ion channel gating with molecular dynamics simulations, Crouzy et al. (1994) calculated that the closing frequency of the *R,R*-linked dimer was 280/s, and that the mean closed time was 0.04 ms when a K^+ ion was present inside the *R,R* dimer. Whereas the calculated value for the mean closed time in the *R,R*-linked dimer is remarkably close to our measurements (Fig. 6), the closing frequency in our experiments was ~40/s. However, and as acknowledged by Crouzy et al. (1994), many different factors could account for variations in the frequency as well as in the duration of closing flickers. The nature of permeating cation, the composition of membrane phospholipids, and water are some of these factors. Indeed, preliminary results from our laboratory show that the permeating ion is critical for flickering. When Na^+ is the conducting ion, for example, gA~D_1~gA remains in the open state without closing flickers at all (Quigley et al., work in progress). This observation contrasts with the existence of flickers in this study as well as with other permeating ions like Cs^+ or Rb^+ (Quigley et al., work in progress). Even though a quantitative characterization was not attempted in this study, PE increased the closing frequency of dioxolane-linked gramicidin A channels. However, natural gA···gA channels also responded to PE by decreasing the mean open time or increasing the closing rate constant (Maer et al., 1997; Neher and Eibl, 1977). It is likely that PE has a general destabilizing effect on open gramicidin A channels.

A novel finding in this study was that the rate of closing flickers increased with voltage, whereas the mean closed duration did not (Fig. 6). Gramicidin channels are usually not voltage dependent (see however Oiki et al., 1995). What causes the voltage dependence of gA~D_1~gA? The structural difference between gA···gA and gA~D_1~gA is caused by the presence of a dioxolane ring in the latter. Because the dioxolane link has low polarizibility, it is not a good candidate for changing its conformation with voltage (Crouzy et al., 1994). However, it is possible that the difference between the total average dipole moments of closed and open gA~D_1~gA is large enough to account for the voltage dependence observed in the mean open times of gA~D_1~gA (see Woolf et al., 1992). It would be of interest to modify the polarity of the basic dioxolane ring, and to

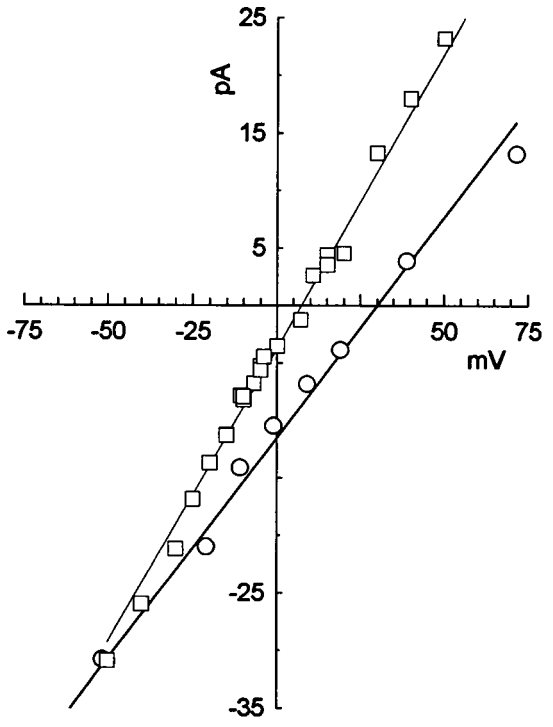

FIGURE 10 Single-channel *I-V* curves in asymmetrical HCl solutions. Circles and squares were obtained with 846 mM//250 mM, and 1455 mM//1000 M HCl gradients (bulk concentrations are given), respectively. Calculated equilibrium electrochemical potentials with these HCl gradients are $E_H = E_{OH} = 31$ mV (○) and 10 mV (□), and $E_{Cl} = -31$ mV (○) and -10 mV (□). Linear regression analysis yielded reversal potentials of ~8 mV (□) and 30 mV (○).

verify whether this change modulates the mean open times of gA~D_1~gA channels.

Proton conductance in gramicidin A channels in different membranes

Proton wire transfer

The higher mobility of protons in liquid water in relation to other ions (Atkins, 1982) cannot be explained by classical diffusion models. Proton translocation in water is often explained by what became known as the Grotthuss mechanism. In this model, translocation of protons in water can be accounted for by 1) breaking hydrogen bonds between water molecules with concurrent release of protons to an adjacent water molecule; 2) establishing new hydrogen bonds between water molecules; 3) reorientation (rotation) of water molecules to the original structure. This is a complex process that involves aggregates of water molecules instead of single water molecules (Agmon, 1995; Pomès and Roux, 1996; Tuckerman et al., 1995). Agmon et al. (1995) proposed that proton transport is actually driven by cleavage and formation of hydrogen bonds in the second solvation shell of $(H_3O)^+$. Translocation of protons in water is thought of as the result of two complementary processes: 1) a sequential hopping of protons between different water aggregates ($k \approx 2.4 \times 10^{11}$ s^{-1}, ion propagation), and 2) restoration of the initial configuration of network of water molecules, which only then will be primed to transport another proton in the same direction ($k \approx 10^{10}$ s^{-1}, propagation of crystal or bonding defect; Nagle and Tristam-Nagle, 1983). It should be noticed however, that the Grotthuss mechanism may not account entirely for proton diffusion at high $[H^+]_0$. It has been suggested that at high acid concentrations, proton diffusion occurs via conventional hydrodynamic mobility of $(H_3O)^+$ (Lown and Thirsk, 1971). Because gA···gA channels are water-filled pores (Finkelstein and Andersen, 1981; Finkelstein, 1987; Levitt et al., 1978; Rosenberg and Finkelstein, 1978), and proton conductance in gA···gA is considerably larger than with other cations, it was proposed that the Grotthuss mechanism operates in gramicidin channels (Akeson and Deamer, 1991; Hladky and Haydon, 1972; Myers and Haydon, 1972). Indeed, Levitt et al. (1978; see also Finkelstein, 1987) provided experimental support for this hypothesis by showing that no streaming potential is developed during (proton + water) flow caused by a transmembrane osmotic gradient imposed across gA···gA channels. Therefore, the study of proton currents offers an opportunity to assess the functional status of the column of water molecules inside gramicidin A channels.

Resistance to proton flow in gA channels

The total resistance (R_t) to proton flow in gA can be considered as the sum of two different components: an intrinsic resistance of the channel to proton flow (R_i) and an access or diffusion-limited resistance (R_a), due to proton movement from the bulk solution to the capture radius of the mouth of the pore (Lauger, 1976; Andersen, 1983a–c; Levitt and Decker, 1988). Alterations in proton flow across gA channels are a consequence of changes in either R_i and/or R_a. R_i is determined by properties of proton transfer inside gA (see above). If the permeability of a channel is very high, as is the case with H^+ permeation across gA channels (see Table 1), the flow of protons can be limited by diffusion of H^+ from the bulk solution to the pore opening. Diffusion limitation is usually identified by sublinear be-

TABLE 1 Proton mobilities (μ_H, $cm^2/V \cdot s$)*

Ice at −5°C#	0.80×10^{-3}
Water at 25°C§	3.62×10^{-3}
6 M HCl at 25°C¶	1.22×10^{-3}
gA~D_1~gA in PEPC	0.47×10^{-3}
gA~D_1~gA in GMO	0.70×10^{-3}
gA···gA in PEPC	0.47×10^{-3}
gA···gA in GMO	0.84×10^{-3}; 0.95×10^{-3}‖

*μ_H values for gramicidin A channels were calculated from g^{max} obtained from the linear portion of single channel *I-V* plots, using Eq. 4 in text.
#Kunst and Warman (1980).
§Atkins (1982).
¶See text (Eq. 5).
‖Akeson and Deamer (1991).

havior or voltage-independent currents in *I-V* plots obtained at relatively low concentrations of permeating ions. It is difficult to unequivocally assign a given alteration in the magnitude of proton currents to either R_i or R_a. Some experimental manipulations in this paper caused alterations in proton currents that seem to be consistent (from the qualitative point of view) with alterations in R_a. However, other alterations in proton currents are difficult to reconcile with simple alterations in R_a and are likely to reflect alterations in R_i.

I-V relationships in both gA~D_1~gA and gA···gA had a marked sublinearity at relatively high voltages in PEPC bilayers ($[H^+]_0$: 2.9–1578 mM; see Fig. 8). Even though GMO bilayers were not suitable for recording single-channel currents at high voltages (see Methods), there are indications of sublinearity in gA···gA in GMO membranes at low (<10 mM) HCl concentrations (Akeson and Deamer, 1991; Decker and Levitt, 1988). However, single-channel supralinearity was demonstrated at higher proton concentrations (≥ 100 mM; Akeson and Deamer, 1991). With gA···gA in GMO or diphytanoylphosphatidylcholine membranes, and alkaline metals as permeating ions, Andersen (1983a–c) showed sublinear *I-V* plots at bulk concentrations of 100 mM. However, at higher concentrations (2 M), the *I-V* plots had a marked supralinearity (Andersen, 1983a).

Gramicidin A channels in PEPC bilayers have a significant sublinear behavior in a wide range of HCl concentrations (Fig. 8). An ohmic or supralinear behavior has never been detected in our experiments in PEPC bilayers. The sublinear behavior in PEPC is consistent with the notion that R_a is limiting proton flow in gA~D_1~gA and gA···gA. Interestingly, the voltage-independent component of proton currents in gA~D_1~gA was larger than in gA···gA at $[H^+]_0$ < 1578 mM, indicating that R_a is smaller in gA~D_1~gA. At $[H^+]_0 \geq 1578$ mM, saturating currents were smaller in gA~D_1~gA than in gA···gA. It is difficult to explain this experimental result by assuming that at these higher concentrations R_a in one or both gA channels is changing. Because proton conductance in gA~D_1~gA at $[H^+]_0 \geq 1578$ mM is significantly attenuated at all voltages in relation to gA···gA, it is possible that R_i is increased at those concentrations. Changes in R_i are likely to reflect structural changes in the water-filled pore of gA~D_1~gA.

gA channels in PEPC

In PEPC bilayers, g-$[H^+]_0$ relationships in gA~D_1~gA and gA···gA are essentially the same in the concentration range of 2.9–1250 mM (Fig. 9). This suggests that the organization of water molecules inside the pore, and the propagation of ionic and bonding defects in gA~D_1~gA, are not significantly affected by the addition of a dioxolane ring between gramicidin A monomers in PEPC. Moreover, diffusion limitation effects, which limit proton flow in gA···gA under certain experimental conditions (Levitt and Decker, 1988; see below), also seem not to be affected by the insertion of a dioxolane ring in gA~D_1~gA. However, it is important to notice that proton conductance in gA~D_1~gA is significantly larger than in gA~D_2~gA (Fig. 4), and this may be an indication that the stereochemistry of dioxolane-gramicidin A may have a considerable impact on the dynamics/structure of water molecules inside the channel's pore, with the end result of modulating proton conductance.

An intriguing observation was that at $[H^+]_0 > 1250$ mM ($[H^+]_{bulk} > 6000$ mM), the single-channel proton conductance in gA~D_1~gA (but not in gA···gA) declined appreciably. A possible interpretation for this effect is that the organization of water molecules inside the pore of gA~D_1~gA is strongly modified (for example, a second H^+ could enter the channel at high $[H^+]_0$ and disorganize the water column inside the pore), and/or significant structural changes are occurring in gA~D_1~gA at these extreme conditions in PEPC. It is important to note that the proton mobility in water increases with $[H^+]$ up to a certain concentration, and at higher concentrations (and/or pressures) it decreases (Lown and Thirsk, 1971). This observation by itself cannot explain the observation that there is a decline in proton conductance in gA~D_1~gA but not in gA···gA.

gA channels in GMO

Whereas the conductance-concentration relationships of different gA's were similar in PEPC membranes (with the notable exception of a decline in g for gA~D_1~gA at high $[H^+]_0$), in GMO membranes gA~D_1~gA and gA···gA behaved differently. The concentration dependence of proton conductance was steeper in gA~D_1~gA (1072 pS/M) than in gA···gA (723 pS/M) at the $[H^+]_0$ of 0.01–2 M. One possibility is that R_a in gA~D_1~gA is considerably lower than in gA···gA. (An additional finding in support of this idea comes from saturation of proton currents in PEPC bilayers. At low $[H^+]_0$, the limiting proton current in gA~D_1~gA is considerably larger than in gA···gA (see Fig. 8, *left panels*). This suggests that the access resistance to the channel pore is lower in gA~D_1~gA than in gA···gA (Lauger, 1976; Andersen, 1983a).) Notice, however, that g^{max} in gA···gA was considerably larger than in gA~D_1~gA at high $[H^+]_0$ (Fig. 8). Taken together, these findings cannot simply be interpreted as differences between R_a values in different gA channels only. Even though proton currents in gA channels are significantly determined by R_a (Decker and Levitt, 1988; Levitt and Decker, 1988), it is possible that the intrinsic resistance to proton flow is different between gA~D_1~gA and gA···gA in GMO bilayers.

Comparison of different gA channels in GMO versus PEPC bilayers

In the range of 10–1250 mM, the concentration dependence of proton conductance is linear in GMO bilayers (Fig. 9, and Akeson and Deamer, 1991) and follows a typical adsorption isotherm in PEPC bilayers (similar for gA~D_1~gA and

gA···gA). In this $[H^+]_0$ range, g is considerably larger in PEPC than in GMO bilayers (*insets* in Fig. 9). Because at low $[H^+]_0$, proton conductance in gA channels is limited predominantly by diffusion of protons from bulk solution to the channel's mouth (Levitt and Decker, 1988), and g is considerably higher in PEPC than in GMO, it is conceivable that an additional source of protons for conduction through gA channels must exist in PEPC membranes that is not present with GMO. The larger proton conductance of gA channels in PEPC in relation to GMO could be accounted for by the presence of extra protons available for conduction through the gA pore. One possibility to consider is the following. The high flow of protons through gA channels decreases the local concentration of H^+ at the entrance of the channel (R_a effects). In GMO membranes, H^+ from bulk solution would have to diffuse to the channel's entrance to keep current flowing through gA channels. In PEPC membranes, however, an additional source of protons to the channel's entrance would come from deprotonation of PE and PC that are located close to the channel's mouth. Depletion of H^+ at the channel's mouth would favor deprotonation of phospholipids adjacent to the mouth of gramicidin A channels and provide an additional source of H^+ for permeation through gA channels. Such a mechanism could work if reprotonation of phospholipids close to the mouth of gA channels occurs by a mechanism considerably faster than diffusion of H^+ from bulk solution. Indeed, reprotonation of phospholipids close to the channel entrance occurs mainly from the diffusion of protons from adjacent phospholipids, and not from the bulk solution: the mobility of protons along a PE monolayer is 27.2×10^{-3} cm^2/(V · s) (Teissie et al., 1985), which is considerably larger than proton mobility in different media (see below, Table 1, and Heberle et al., 1994). In summary, depletion of H^+ at the mouth of gA channels causes deprotonation of phospholipids located adjacent to the channel entrance. This, in turn, would add protons to the channel's entrance. Protons dissociated from PE and PC would constitute an extra source of protons contributing to a larger (in relation to GMO membranes) g. In this regard, it is interesting to note that the K_D of g-$[H^+]$ relationships for both gA~D_1~gA and gA···gA in PEPC (Eq. 3) is likely to reflect the binding of H^+ to the membrane rather than to gA. K_D values were ~300 mM (Fig. 9), which is within the range of K_D values measured for different phospholipids (Marsh, 1990). It is important to stress, however, that the mechanism described above could explain only part of the differences between g-$[H^+]_0$ relationships of gA's in GMO versus PEPC bilayers.

Differences between single-channel conductances in PEPC versus GMO due to surface charge effects were accounted for in this study. The concentration of protons at the membrane/solution interface was corrected for protonation of phospholipids, which does not occur with GMO (Fig. 2). Although uncertainties may exist regarding the precise location of the mouth of different gramicidin A channels in relation to the plane of the bilayer, the qualitative nature of the conclusions in this paper holds. It is clear that the significant differences found between proton conductions in gramicidin A channels in different bilayers cannot be explained by surface charge effects only.

Finally, it is important to add that the decline in single-channel proton conductance at $[H^+]_0 > 1250$ mM was not present in GMO bilayers. It is difficult to account for this result on the basis of diffusion limitation problems only.

Proton mobilities in solution and in different gA's

It is instructive to calculate the mobility of protons from the linear portion of *I-V* plots (Fig. 8). In saturating conditions (g^{max}), the proton mobility (μ_H, cm^2/(V · s)) in different gramicidin A channels under a constant electric field can be calculated by

$$\mu_H = L^2 * g^{max}/e \quad (4)$$

where L is the length of the gramicidin A pore (25×10^{-8} cm), and e is the elementary charge. With g^{max} values taken from Fig. 9, Eq. 4 yields values for μ_H (see Table 1) ranging from 0.47×10^{-3} (both gramicidin A channels in PEPC bilayer) to ~0.90×10^{-3} cm^2/(V · s) (gA···gA in GMO; see Table 1). Note that the calculated μ_H is an "average" mobility that reflects a combination of different proton mobilities in solution, at the (membrane + gramicidin)/solution interface, and in the gramicidin pore itself. How do these μ_H values compare with other measurements of proton mobilities in different conditions? Table 1 lists proton mobilities in water at 25°C (3.62×10^{-3} cm^2/(V · s)) and in ice (0.8×10^{-3} cm^2/(V · s) at −5°C; see Kunst and Warman, 1980). μ_H values in different gramicidin A channels and bilayers are comparable with proton mobilities in pure water. However, an even better agreement is obtained when we compare μ_H values in gramicidin A and HCl. (The mobilities of protons in different HCl solutions were calculated from a combination of the Einstein and Nernst-Einstein equations, $\mu_H = \lambda_{HCl} \times t_H/(z \times F)$, where λ_{HCl} is the equivalent conductance of an HCl aqueous solution (S/M), and t_H is the transference number for protons, which is equal to $[\lambda_H/(\lambda_H + \lambda_{Cl})]$. t_H is 0.84 for concentrated HCl solutions (Robinson and Stokes, 1959, table 7.7), and λ_{HCl} has been measured in a wide range of HCl concentrations (Weast, 1989, p. D-167). Note that μ_H in (solution + gramicidin A in GMO) is ~75% of the proton mobility in 6 M HCl. It is remarkable that gramicidin A channels do not offer an appreciable resistance to proton translocation. It is possible that protons cross different gramicidin A channels in different bilayers with a minimum of direct interaction with the channel itself. Finally, it is important to stress the similarity between proton mobilities in ice and in different gA's.

Proton translocations in water and across biological membranes are essential but poorly understood phenomena in biology and physical chemistry. The complexity of this problem led to the development of simple model systems that have been used to help understand proton translocation across lipid bilayers (Akeson and Deamer, 1991; Deamer

and Nichols, 1989; Paula et al., 1996; Prabhananda and Kombrabail, 1996; see Nagle and Tristam-Nagle, 1983). This study clearly demonstrates that lipid bilayers have a significant impact on proton translocation across gramicidin A channels. One possibility is that proton translocation across membrane proteins might be generally influenced by the composition of lipid bilayers.

We thank Ms. Paulene Quigley for help with the organic synthesis and Dr. Stephen B. Jones for sharing the use of his high-performance liquid chromatography. We also thank Dr. Stefan H. Heinemann for making available to us his doctoral dissertation, and Drs. Noam Agmon, Duan Chen, and Robert S. Eisenberg for stimulating discussions and for suggesting notations used for different gramicidin A dimers. We are indebted to the reviewers of this paper for their truly insightful comments.

This work was supported in part by Loyola University Medical Center (SC). EPQ had a fellowship awarded by the Dean's Office of Loyola Medical School and is currently a Schmitt fellow of Loyola University Chicago.

REFERENCES

Agmon, N. 1995. The Grotthuss mechanism. *Chem. Phys. Lett.* 244: 456–462.

Agmon, N., S. Y. Goldberg, and D. Huppert. 1995. Salt effect on transient proton transfer to solvent and microscopic proton mobility. *J. Mol. Liquids.* 64:161–195.

Akeson, M., and D. W. Deamer. 1991. Proton conductance by the gramicidin water wire. Model for proton conductance in the F_0F_1ATPases? *Biophys. J.* 60:101–109.

Andersen, O. S. 1983a. Ion movement through gramicidin A channels. Single channel measurements at very high potentials. *Biophys. J.* 41: 119–133.

Andersen, O. S. 1983b. Ion movement through gramicidin A channels. Interfacial polarization effects on single channel current measurements. *Biophys. J.* 41:135–146.

Andersen, O. S. 1983c. Ion movement through gramicidin A channels. Studies on the diffusion-controlled association step. *Biophys. J.* 41: 147–165.

Andersen, O. S. 1984. Gramicidin channels. *Annu. Rev. Physiol.* 46: 531–548.

Andersen, O. S., and R. E. Koeppe, II. 1992. Molecular determinants of channel function. *Physiol. Rev.* 72:S89–S158.

Arseniev, A. S., I. L. Barsukov, V. F. Bystrov, A. L. Lonize, and Y. A. Ovchinikov. 1985. Proton NMR study of gramicidin A transmembrane ion channel. Head-to-head right handed, single stranded helices. *FEBS Lett.* 186:168–174.

Atkins, P. W. 1982. Physical Chemistry, 2nd Ed. Oxford University Press, Oxford.

Bamberg, E., and K. Janko. 1977. The action of a carbonsuboxide dimerized gramicidin A on lipid bilayer membranes. *Biochim. Biophys. Acta.* 465:486–499.

Busath, D. D. 1993. The use of physical methods in determining gramicidin channel structure and function. *Annu. Rev. Physiol.* 55:473–501.

Busath, D., and G. Szabo. 1981. Gramicidin forms multi-state rectifying channels. *Nature.* 294:371–373.

Bystrov, V. F., and A. S. Arseniev. 1988. Diversity of the gramicidin A spatial structure: two dimensional ^{1}H NMR study in solution. *FEBS Lett.* 44:925–940.

Crouzy, S., T. B. Woolf, and B. Roux. 1994. A molecular dynamics study of gating in dioxolane-linked gramicidin A channels. *Biophys. J.* 67: 1370–1386.

Cukierman, S. 1991. Asymmetric electrostatic effects on the gating of rat brain sodium channels in planar lipid membranes. *Biophys. J.* 61: 845–856.

Cukierman, S. 1993. Barium modulates the gating of BTX-treated Na^+-channels in high ionic strength solutions. *Biophys. J.* 65:1168–1173.

Deamer, D. W., and J. W. Nichols. 1989. Proton flux mechanisms in model and biological membranes. *J. Membr. Biol.* 107:91–103.

DeCoursey, T. E., and V. V. Cherny. 1994. Voltage-activated hydrogen ion currents. *J. Membr. Biol.* 141:203–223.

DeCoursey, T. E., and V. V. Cherny. 1997. Deuterium isotope effects on permeation and gating of proton channels in rat alveolar epithelium. *J. Gen. Physiol.* 109:415–434.

Decker, E. R., and D. G. Levitt. 1988. Use of weak acids to determine the bulk limitation of H^+ ion conductance through the gramicidin channel. *Biophys. J.* 53:25–32.

Eigen, M., and L. DeMaeyer. 1958. Self-dissociation and protonic charge transport in water and ice. *Proc. R. Soc. Lond. A.* 247:505–533.

Finkelstein, A. 1970. Weak-acid uncouplers of oxidative phosphorylation. Mechanism of action on thin lipid membranes. *Biochim. Biophys. Acta.* 205:1–6.

Finkelstein, A. 1987. Water Movement Through Lipid Bilayers, Pores, and Plasma membrane. Theory and Reality. John Wiley, New York.

Finkelstein, A., and O. S. Andersen. 1981. The gramicidin A channel: a review of its permeability characteristics with special reference to the single-file aspect of transport. *J. Membr. Biol.* 39:155–171.

Heberle, J., J. Riesle, G. Thiedemann, D. Oesterhelt, and N. A. Dencher. 1994. Proton migration along the membrane surface and retarded surface to bulk transfer. *Nature.* 370:379–382.

Heinemann, S. H. 1990. Untersuchung interner bewegungen von kanalbildenden proteinen mit elektrophysiologischen methoden und kraftfeldrechnungen. Dissertation, University of Göttingen, Göttingen, Germany.

Hladky, S. B., and D. A. Haydon. 1972. Ion transfer across lipid membranes in the presence of gramicidin A. I. Studies of the unit conductance channel. *Biochim. Biophys. Acta.* 274:294–312.

Hladky, S. B., and D. A. Haydon. 1984. Ion movements in gramicidin channels. *Curr. Top. Membr. Transp.* 21:327–372.

Israelachvili, J. N. 1992. Intermolecular and Surface Forces, 2nd Ed. Academic Press, London.

Jordan, P. C. 1987. Microscopic approach to ion transport through transmembrane channels. The model system gramicidin. *J. Phys. Chem.* 91:6582–6591.

Junge, W. 1989. Protons, the thylakoid membrane, and the chloroplast ATP synthase. *Ann. N.Y. Acad. Sci.* 574:268–285.

Ketchem, R. R., W. Hu, and T. A. Cross. 1993. High resolution of gramicidin A in a lipid bilayer by solid-state NMR. *Science.* 261: 1457–1460.

Koeppe, R. E., II, and O. S. Andersen. 1996. Engineering the gramicidin channel. *Annu. Rev. Biophys. Biomol. Struct.* 25:231–258.

Kunst, M., and J. M. Warman. 1980. Proton mobility in ice. *Nature.* 288:465–467.

Lauger, P. 1976. Diffusion-limited ion flow through pores. *Biochim. Biophys. Acta.* 455:493–509.

Levitt, D. G. 1984. Kinetics of movement in narrow channels. *Curr. Top. Membr. Transp.* 21:181–197.

Levitt, D. G., and E. R. Decker. 1988. Electrostatic radius of the gramicidin channel determined from voltage dependence of H^+ ion conductance. *Biophys. J.* 53:33–38.

Levitt, D. G., S. R. Elias, and J. M. Hautman. 1978. Number of water molecules coupled to the transport of sodium, potassium, and hydrogen ions via gramicidin nonactin or valinomycin. *Biochim. Biophys. Acta.* 512:436–451.

Lown, D. A., and H. R. Thirsk. 1971. Proton transfer conduction in aqueous solution. Part 2. Effect of pressure on the electrical conductivity of concentrated orthophosphoric acid in water at 25°C. *Trans. Faraday Soc.* 67:149–152.

Maer, A. M., L. L. Providence, and O. S. Andersen. 1997. The effective size of lipid polar head groups and gramicidin channel function. *Biophys. J.* 72:A191 (Abstr.).

Marsh, D. 1990. CRC Handbook of Lipid Bilayers. CRC Press, Boca Raton, FL. 81–85.

Myers, V. B., and D. A. Haydon. 1972. Ion transfer across lipid membranes in the presence of gramicidin A. *Biochim. Biophys. Acta.* 274:313–322.

Nagle, J. F., and H. J. Morowitz. 1978. Molecular mechanisms for proton transport in membranes. *Proc. Natl. Acad. Sci. USA.* 75:298–302.

Nagle, J. F., and S. Tristam-Nagle. 1983. Hydrogen bonded chain mechanisms for proton conduction and proton pumping. *J. Membr. Biol.* 74:1–14.

Neher, E., and H. Eibl. 1977. The influence of phospholipid polar groups on gramicidin channels. *Biochim. Biophys. Acta.* 464:37–44.

Oiki, S., Koeppe, R. E., II, and O. S. Andersen. 1995. Voltage-dependent gating of an asymmetric gramicidin channel. *Proc. Natl. Acad. Sci. USA.* 92:2121–2125.

Paula, S., A. G. Volkov, A. N. Van Hoek, T. H. Haines, and D. W. Deamer. 1996. Permeation of protons, potassium ions, and small polar molecules through phospholipid bilayers as a function of membrane thickness. *Biophys. J.* 70:339–348.

Pomès, R., and B. Roux. 1996. Structure and dynamics of a proton wire: a theoretical study of H^+ translocation along the single-file water chain in the gramicidin A channel. *Biophys. J.* 71:19–39.

Pomès, R., and B. Roux. 1997. Free energy profiles governing H^+ conduction in proton wires. *Biophys. J.* 72:A246 (Abstr.).

Prabhananda, B. S., and M. H. Kombrabail. 1996. Two mechanisms of H^+/OH^- transport across phospholipid vesicular membrane facilitated by gramicidin A. *Biophys. J.* 71:3091–1097.

Ring, A. 1986. Brief closures of gramicidin A channels in lipid bilayer membranes. *Biochim. Biophys. Acta.* 856:646–653.

Robinson, R. A., and R. H. Stokes. 1959. Electrolyte Solutions, 2nd Ed. Butterworths, London.

Rosenberg, P. A., and A. Finkelstein. 1978. Interaction of ions and water in gramicidin A channels. Streaming potentials across lipid bilayer membranes. *J. Gen. Physiol.* 72:327–340.

Sarges, R., and B. Witkop. 1965. V. The structure of valine- and isoleucine-gramicidin A. *J. Am. Chem. Soc.* 87:2011–2019.

Sigworth, F. J., D. W. Urry, and K. U. Prasad. 1987. Open channel noise. III. High resolution recordings show rapid current fluctuations in gramicidin A and four chemical analogues. *Biophys. J.* 52:1055–1064.

Stankovic, C. J., S. H. Heinemann, J. M. Delfino, F. J. Sigworth, and S. L. Schreiber. 1989. Transmembrane channels based on tartaric acid-gramicidin A hybrids. *Science.* 244:813–817.

Stankovic, C. J., S. H. Heinemann, and S. L. Schreiber. 1990. Immobilizing the gate of a tartaric acid-gramicidin A hybrid channel molecule by rational design. *J. Am. Chem. Soc.* 112:3702–3704.

Teissie, J., M. Prats, P. Soucaille, and J. F. Tocanne. 1985. Evidence for conduction of protons along the interface between water and a polar lipid monolayer. *Proc. Natl. Acad. Sci. USA.* 82:3217–3221.

Tuckerman, M., K. Laasonen, M. Sprik, and M. Parrinello. 1995. *Ab initio* dynamics simulation of the solvation and transport of hydronium and hydroxyl ions in water. *J. Chem. Phys.* 103:150–161.

Urry, D. W. 1971. Gramicidin A transmembrane channel: a proposed $\pi_{(L,D)}$ helix. *Proc. Natl. Acad. Sci. USA.* 68:672–676.

Urry, D. W., M. C. Goodall, J. D. Glickson, and D. F. Meyers. 1971. The gramicidin A transmembrane channel: characteristics of head-to-head dimerized $\pi_{(L,D)}$ helices. *Proc. Natl. Acad. Sci. USA.* 68:1907–1911.

Wallace, B. A. Gramicidin channels and pores. 1990. *Annu. Rev. Biophys. Biophys. Chem.* 19:127–157.

Weast, R. C. 1989. Handbook of Chemistry and Physics. CRC Press, Boca Raton, FL.

Woolf, T., S. Crouzy, B. Roux, T. Simonson, S. Heinemann, and F. Sigworth. 1992. Molecular dynamics calculations of water behaviour and applied voltage effects on dioxolane-ring linked gramicidin. *Biophys. J.* 61:A526 (Abstr.).